Bidirectional microbial electron transfer: switching an acetate oxidizing biofilm to nitrate reducing conditions

Narcís Pous, Alessandro Carmona Martinez, Anna Vilajeliu-Pons, Erika Fiset, Lluis Bañeras, Eric Trably, M. Dolors Balaguer, Jesus Colprim, Nicolas Bernet, Sebastià Puig

Bidirectional microbial electron transfer: switching an acetate oxidizing biofilm to nitrate reducing conditions

Narcís Pous[a], Alessandro A. Carmona-Martínez[b], Anna Vilajeliu-Pons[a], Erika Fiset[a], Lluis Bañeras[c], Eric Trably[b], M. Dolors Balaguer[a], Jesús Colprim[a], Nicolas Bernet[b] and Sebastià Puig[a,*]

[a]LEQUiA, Institute of the Environment, University of Girona, C/ Maria Aurèlia Capmany, 69, Facultat de Ciències, E-17071 Girona, Spain. *Correspondence to: S. Puig, E-mail: sebastia@lequia.udg.cat

[b]INRA, UR0050, Laboratoire de Biotechnologie de l'Environnement, Avenue des Etangs, Narbonne, F-11100, France

[c]Molecular Microbial Ecology Group, Institute of Aquatic Ecology, University of Girona, Spain.

ABSTRACT

Up to date a few electroactive bacteria embedded in biofilms are described to catalyze both anodic and cathodic reactions in bioelectrochemical systems (i.e. bidirectional electron transfer). How these bacteria transfer electrons to or from the electrode is still uncertain. In this study the extracellular electron transfer mechanism of bacteria within an electroactive biofilm was investigated by using cyclic voltammetry (CV) and differential pulse voltammetry (DPV). First, a mature anodic electroactive biofilm was developed from an activated sludge sample (inoculum), acetate as electron donor and a poised electrode (+397 mV vs. SHE). Later, this biofilm was "switched" to biocathodic conditions by feeding it with a medium containing nitrates and poising the electrode at –303 mV vs. SHE. The electrochemical characterization indicated that both, acetate oxidation and nitrate reduction took place at a similar formal potential of -175±05 and -175±34 mV vs. SHE, respectively. The biofilm was predominantly composed by *Geobacter* sp. at both experimental conditions. Taken together, the results indicated that both processes could be catalyzed by using the same electron conduit, and most likely by the same bacterial consortium. Hence, this study suggests that electroactive bacteria

within biofilms could use the same electron transfer conduit for catalyzing anodic and cathodic reactions.

Keywords

Bidirectional extracellular electron transfer, bioanode, biocathode, bioelectrochemical systems, electroactive biofilms.

1. INTRODUCTION

The interaction of microorganisms with metals, such as dissimilatory Fe(III) reduction (Lovley, 1991) has found a substantial utility for microbial bioelectrochemical systems (BES) (Pant et al., 2012). In BES, strains within the well-known dissimilatory metal reducing *Geobacteraceae* (Bond and Lovley, 2003) and *Shewanellaceae* (Baron et al., 2009) bacterial families, are capable of oxidizing and reducing a solid electrode material. In bioanodes, bacteria use the electrode as an electron sink for the oxidation of organic matter. Thus, electrical energy can be harvested (Logan and Rabaey, 2012). Contrarily, in biocathodes, bacteria obtain electrons from the electrode to reduce oxidized compounds. Such electrode oxidizing process can be used for treating inorganic contaminants, such as nitrate (Clauwaert et al., 2007), or to produce added-value chemicals like hydrogen (Batlle-Vilanova et al., 2014) or C2-C4 organic acids and alcohols (Ganigue et al., 2015), among others.

Metal-reducing bacteria use external cytochromes or soluble mediators to interact with metals via a process termed direct and mediated electron transfer (DET and MET, respectively) (Schröder, 2007). In BES, the electron transfer between microorganisms and bioanodes has been well elucidated for a handful of anode-respiring bacteria (ARB) such as *Geobacter sulfurreducens* (Fricke et al., 2008), *Rhodopseudomonas palustris* (Xing et al., 2008), *Thermincola ferriacetica* (Parameswaran et al., 2013),

Geoalkalibacter subterraneus (Carmona-Martínez et al., 2013), and *Shewanella oneidensis* (Marsili et al., 2008). While bacteria within the *Geobacteraceae* are examples of ARB using DET to transport electrons from an available electron donor (organic matter) to the solid electrode (Carmona-Martínez et al., 2013; Fricke et al., 2008), members of the *Shewanellaceae* have been characterized for using both DET and MET (Carmona-Martinez et al., 2011; Marsili et al., 2008). However, the *Shewanellaceae* produce significantly less current densities. In contrast, the fundamental principles of the mechanism for electron uptake from cathodes by microorganisms have been scarcely reported (Rosenbaum et al., 2011). Few examples of biocathode electron transfer characterization are available in literature. *Mariprofundus ferrooxydans* was electrochemically characterized for its ability of reducing oxygen using an electrode as electron donor (Summers et al., 2013). Recently, two independent works have reported the electrochemical characterization of nitrate reducing biocathodes, one being predominantly colonized by *Thiobacillus* sp. (Pous et al., 2014), and the second one being dominated by *Rhodocyclales* and *Burkholderiales*, also within the *betaproteobacteria* (Gregoire et al., 2014). These articles described Nernstian current-potential dependency for biocathode, as it is usually observed in bacterial bioanodes.

For metal-reducing bacteria able to both reduce Fe(III) and oxidize Fe(II) it has been hypothesized that the same protein of the Mtr respiratory pathway could be used for a bidirectional transport of electrons, i.e. obtaining and delivering electrons from/to the electrode (Shi et al., 2012).

In BES, the bidirectional activity of a few electroactive bacteria embedded in biofilms has been demonstrated. Dumas et al. (2008) and Strycharz et al. (2011) showed that *Geobacter sulfurreducens* could perform anodic acetate oxidation and cathodic

fumarate reduction, but their results suggested that a different electron conduit was used. Ross et al. (2011) demonstrated that *Shewanella oneidensis* Mtr pathway could be reversed for fumarate reduction. Geelhoed and Stams (2011) showed the ability of pure *Geobacter sulfurreducens* to use the electrode for both the oxidation of acetate and the reduction of protons to hydrogen. Jeremiasse et al. (2012) showed that a mixed culture biofilm could be firstly grown as an acetate-oxidizing bioanode and afterwards switched to a hydrogen-producing biocathode, which certainly decreased the start-up time (>2 times faster). Mixed culture biofilms able to both catalyze organic matter oxidation and oxygen or nitrate reduction have been also described (Blanchet et al., 2014; Cheng et al., 2012, 2010). However, to the best of the authors' knowledge, the main electron transfer mechanism governing such "switchable" electroactive biofilms has not been elucidated yet. For this reason, this study presents the electrochemical characterization of a "switchable" electroactive biofilm able to oxidize acetate and later able to successfully reduce nitrate.

Two anodic electroactive biofilms were developed from an activated sludge sample, using acetate as sole electron donor and a polarized electrode at +397 mV vs standard hydrogen electrode (SHE) as sole electron acceptor. Once the biofilm was visible in the anode (after three fed-batch cycles), its operation was switched to a biocathode able to reduce nitrates using the electrode as electron donor at –303 mV vs. SHE. The electron transfer mechanism of both oxidizing- and reducing-activities was elucidated using voltammetric techniques.

2. MATERIAL AND METHODS

2.1. Experimental set-up

A three-neck 1L round-bottom flask (one-chamber BES) was used as a reactor and assembled following a three-electrode arrangement. Two graphite rods (diameter: 4.5 mm and length: 250 mm) were used as working- and counter- electrodes, respectively (Mersen Iberica, Spain). All bioelectrochemical experiments were conducted under potentiostatic control using Ag/AgCl as a reference electrode (+197 mV vs SHE, model RE-5B BASi, United States). The working electrode was placed at the central neck, while the reference- and the counter- electrodes were placed at lateral necks.

Two biological replicates were performed using the same set-up (labeled as R-1 and R-2, respectively), as well as an abiotic control test.

All media were prepared with distillated water and vigorously flushed with N_2 gas (purity ≥ 99.9%; Praxair, Spain) to remove traces of dissolved oxygen. Basal (substrate free solution) mineral media were composed of: 2.640g·L^{-1} KH_2PO_4, 4.320g·L^{-1} Na_2HPO_4; 0.130g·L^{-1} KCl; 0.020g·L^{-1} NH_4Cl and 0.1mL micronutrients (Carmona-Martínez et al., 2013). Basal media was amended with acetate (CH_3COO^-, 0.840g·L^{-1} CH_3COONa) or nitrate plus bicarbonate (NO_3^-, 0.182g·L^{-1} $NaNO_3$ and 1.398g·L^{-1} $NaHCO_3$) for bioanode or biocathode conditions, respectively. The round-bottom flask was filled with 1L of medium, which resulted in a working electrode wet surface area of 31±1 cm^2 for R-1 and R-2. All experiments were carried out at pH 7.0 and room temperature (22ºC).

2.2. Reactor operation: Bioanodic and biocathodic conditions

The round-bottom flask was inoculated with 0.050 L of activated sludge from an urban wastewater treatment plant (Girona, Spain) per 1 L of synthetic medium. Figure 1 shows the workflow followed in this study.

An electroactive bioanode was grown by feeding the reactor with the acetate-containing medium. The reactor was operated in fed-batch mode for three different fed-batch cycles in which the acetate-exhausted medium was replaced for fresh medium containing the initial amount of acetate. At all times during anodic conditions, the working electrode (WE) was polarized at +200 mV vs Ag/AgCl (+397 mV vs SHE at 25ºC) (model SP-50, Bio-logic, France) following the procedure described elsewhere (Gimkiewicz and Harnisch, 2013). Henceforth, all potentials will be referred vs SHE.

Once the electrochemical characterization of mature anodic biofilms concluded (see below) the medium was changed to a nitrate-solution to start biocathodic conditions and two feeding cycles were performed. During biocathodic conditions, the WE was polarized at -303 mV.

The procedure was performed in duplicate (R-1 and R-2). Abiotic nitrate reduction was tested using new graphite electrodes polarized at -303 mV during 16 h.

2.3. Characterization of biofilm performance: Bioelectrochemical measurements

The biofilm was electrochemically characterized by cyclic voltammetry (CV) under turnover, acetate (CH_3COO^-) or nitrate (NO_3^-), and non-turnover (substrate-free) conditions. The CV was performed from -401 to +798 mV at scan rate of $1 mV \cdot s^{-1}$ (Harnisch and Freguia, 2012). Additionally, differential pulse voltammetry (DPV) was recorded from -401 to +798 mV by setting the following parameters: pulse height of 50 mV, pulse width of 300 ms, step height of 1 mV and step time of 1000 ms (scan rate of $1 mV \cdot s^{-1}$). Data extracted from CVs and DPVs as peak detection and first derivative analyses were performed using the free-software SOAS (Fourmond et al., 2009). The mid-point potential (E_f) of redox couples was calculated as the mean value of the oxidative and reductive potential. All data are based on experiments of at least two independent biofilm replicates and standard deviations are presented throughout the

manuscript. The use of two biologic replicates have been stated as enough to prove bioelectrochemical performance (Logan, 2012).

2.3. Analytical methods and calculations

At the start and at the end of each feeding period, samples were taken for physicochemical analyses. The biofilm activity under bioanodic conditions was checked by the analysis of acetate and any other short chain volatile fatty acid: propionic, butyric, isobutyric, valeric, isovaleric, hexanoic, ethanol) in the liquid phase through a gas-chromatograph equipped with a DB-FFAP column and a flame ionization detector (7890A, Agilent, USA). The biofilm activity under biocathodic contidions was checked by the analysis of nitrates (electron acceptor) and nitrites, ammonium and nitrous oxide (possible end-products). Nitrates, nitrites and ammonium were analysed following the recommendations of the American Public Health Association (APHA) (APHA, 2005). Nitrous oxide was analysed using a N_2O microsensor (Unisense, Denmark). pH was measured with a pH-meter (pH-meter basic 20^+, Crison, Spain). Coulombic efficiency (*CE*) for nitrate reduction was calculated following the methodology described by Virdis et al. (2009).

2.4. Molecular analyses

Once both bioanodic and biocathodic conditions were electrochemically characterized, a representative sample of the biofilm attached to the electrode was gently scratched, collected and stored at -20ºC. Bacterial 16S rRNA gene was amplified by PCR using universal primers 357F-GC (Turner et al., 1999) and 907R (Lane, 1991). PCR products were analyzed by Denaturing Gradient Gel Electrophoresis (DGGE) according to the method described by Prat et al. (2009). A 35–70% urea-formamide denaturing gradient was used (Supplementary material S1). The DGGE gels were stained with SybrGold during 45 minutes and visualized under UV excitation. Digital images of acrylamide

gels were used to determine the relative intensity of each band (a proxy for its relative abundance) by using ImageJ software (National Institutes of Health (NIH), USA). Nucleotide sequences obtained from selected DGGE bands were aligned with available 16S rRNA genes of known *Geobacter* species available in the Silva data base (www.arb-silva.de, downloading date February 2015). Phylogenetic trees were reconstructed with distance (neighbor-joining, NJ) and maximum-parsimony (MP) methods using MEGA v6.06 software with 1000 bootstrap replicates (Tamura et al., 2013). Pairwise deletion and Jukes Cantor methods were used. NCBI accession numbers of *Geobacteraceae* used can be found in supplementary material S2.

3. RESULTS AND DISCUSSION

3.1. Growth of an electroactive anodic biofilm

Reactor inoculation and anodic biofilm growth were carried out following the standard procedure described elsewhere (Gimkiewicz and Harnisch, 2013). Such protocol is as an effective methodology to grow an electroactive biofilm dominated by *Geobacter* sp. when using activated sludge as inoculum (Harnisch et al., 2011; Liu et al., 2008). The growth of a *Geobacter* sp. enriched biofilm on the two replicates was inferred due to the appearance of its characteristic visible reddish colour on the working-electrode surface (later confirmed by sequencing). It is worth noticing that no biofilm was observed on the counter-electrode surface, which supports that the reddish biofilm observed on the working-electrode was related to its behaviour. However, electroactivity was slightly higher for R-1 in terms of maximum current density (j_{max}) probably due to the higher biomass in this electrode compared to R-2 (Image of R-1 showed in supplementary material S3).

Nonetheless, three fed-batch cycles were conducted at +397 mV to ensure that a mature anodic biofilm able to oxidize acetate was grown on the electrodes. Representative fed-batch cycles for R-2 can be observed in Figure 2. Representative cyclic voltammetries are shown in Figure 2 for R-1 and in supplementary material S4 for R-2. Once the development of the electroactive biofilm was corroborated by reproducible values of j_{max} and a stable shape in cyclic voltammetry, the activity of the biofilm was "switched" from anodic to cathodic conditions by poising the working electrode at -303 mV.

3.1.1. Turnover CV analyses of mature anodic acetate-oxidizing biofilms

The anodic activity in the presence of acetate (*i.e.*, "turnover conditions") was characterized through cyclic voltammetry (CV). Representative CVs of mature

electroactive biofilms are shown in Figure 3 compared to the bare electrode CV. Electrochemical data extracted from CVs for both replicates are summarized in Table 1.

It is worth noticing that the CV performed under turnover conditions was clearly different from the one of the bare electrode abiotic voltammogram (flat black CV in Fig. 2). Thus, such turnover CV indicated the establishment of a mature biofilm. Furthermore, the CV under turnover conditions presented a positive sigmoidal shape typically observed in biofilms colonized by anode-respiring bacteria (ARB) able to produce repetitive high currents (*i.e.*, j around 1 $A \cdot m^{-2}$) and thick biofilms (Fricke et al., 2008). It additionally suggests a DET mechanism (Carmona-Martínez et al., 2013). The sigmoidal shape was further characterized by calculating the first derivative of the current with respect to the applied electrode potential during CV (Inset in Fig. 3A). The biofilm in both replicates was characterized by the detection of a dominant redox couple with a formal potential $E_{f,1}$ around -175±5 mV (Table 1).

3.1.2. Non-turnover CV and DPV analyses of mature anodic biofilms

A typical CV of non-turnover conditions could be observed when substrate-free medium was used (Fig. 3B). DPV was used as an additional voltamperometric technique to clarify the catalytic activity under non-turnover conditions (Harnisch and Rabaey, 2012). Experimentally, DPV is considered to possess a higher degree of selectivity/sensitivity to study electroactive biofilms (Marsili et al., 2008). non-turnover DPVs showed a clear peak at around -159±22 mV. Interestingly, this DPV peak matched to the formal potential $E_{f,1}$ previously observed in CV recorded under acetate-containing medium (turnover conditions). This finding suggests that the biofilm could be employing a similar electron transfer mechanism under both turnover and non-turnover conditions.

A further comparison of $E_{f,1}$ showed its proximity to the value previously reported by Liu et al., (2008) (-124 mV vs. SHE) (Liu et al., 2008) where the authors developed an electroactive biofilm highly enriched in *Geobacter* sp. from a primary wastewater as inoculum and using acetate as the electron donor. Such experimental procedure was very similar to the one used in this study. Additionally, $E_{f,1}$ was similar to values reported in pure cultures of *Geobacter sulfurreducens* with E_f between -106 and -206 mV vs. SHE. This evidences a possible shared direct electron transfer mechanism (Carmona-Martínez et al., 2013).

The comparison of CV shapes (considered as equivalent to an electrochemical fingerprint of certain microorganisms), the formal potentials using acetate as electron donor, and the reddish biofilm observed at the end of the three feeding cycles (supplementary material S3) suggest that the biofilm grown on the electrode was mainly composed by an anode-respiring bacterium belonging to the *Geobacteraceae* family (Harnisch et al., 2011; Liu et al., 2008).

Under non-turnover CV conditions an oxidation peak at around +91 mV was also found which could indicate the presence of a masked redox couple (Fig. 2B). The use of DPV revealed a "shoulder" on the voltammogram that somehow resembles a minor redox peak at about +183±2 mV vs. SHE. Nevertheless, it is not completely clear how this non prominent additional peak ($E_{f,2}$) is involved in the overall ET mechanism.

3.2. Switching the anodic electroactive biofilm to denitrifying cathodic activity

After three fed-batch cycles operated with acetate as sole electron donor were completed, the denitrifying activity of the electroactive biofilm was tested (Fig. 2). The acetate exhausted medium was removed and the reactor was fed with a nitrate-containing medium (32.1±0.9 mgN-NO_3^-·L^{-1}). To promote denitrification, the electrode potential was switched from +397 to a more reductive value, -303 mV, since at this

potential the denitrifying cathodic catalytic activity is clearly enhanced (Pous et al., 2015, 2014).

After the exchange of medium and the decrease of the WE potential, it took about two days for a constant negative current density to occur as an indication of electron uptake (Fig. 1 on day 65^{th}). Concomitantly, the concentrations of nitrate, nitrite and nitrous oxide were analyzed at the beginning and at the end of each fed cathodic cycle to corroborate nitrate reducing activity. According to the chemical analyses conducted, nitrate reduction occurred without accumulation of intermediates (nitrite or nitrous oxide), with an average nitrate removal rate of 345±166 $mgN \cdot m^{-2} \cdot d^{-1}$ considering the whole batch (supplementary material S5). The maximum nitrate removal rate was observed in R-1 with 532 $mgN \cdot m^{-2} \cdot d^{-1}$ (218 $mgN \cdot m^{-2} \cdot d^{-1}$ for R-2). Abiotic experiments were carried out during 16 hours in which a stable but very low current density of -0.003±0.000 $A \cdot m^{-2}$ was observed and no nitrate reduction could be detected as an experimental evidence of the biofilm mediated electrochemical activity observed in R-1 and R-2. No conversion of nitrite neither nitrous oxide were observed in abiotic experiments.

According to our results, the microbial community within the electroactive biofilm was able to reduce nitrates. Considering that the current demand observed was used for the whole denitrification pathway (from NO_3^- to N_2, which counts as 5 mol of electrons per mol of NO_3^-), the mean *CE* was 14±1%. If only the reduction of nitrate to nitrite was taken into account (which accounts for $2e^-$ per mol of NO_3^-), the *CE* was 35±4%.

3.2.1. Turnover CV analyses of cathodic denitrifying biofilms

Besides the current uptake during the chronoamperometry (Fig. 2) and the conversion of nitrate into dinitrogen gas, the biofilm activity in the presence of nitrate was also

electrochemically characterized by CV (Fig. 3C). The CVs in the presence of nitrate revealed that the anodic biofilm originally developed with acetate was able to switch to nitrate-reducing conditions, presenting a negative sigmoidal shape. When calculating the first derivative of such cathodic turnover CVs, a clear redox couple was observed with a formal potential at -175±34 mV (pH 7.0 and 22ºC). The mid-point potential for nitrate reduction is similar to previous values reported for denitrifying biocathodes. For example, Pous et al. (2014) reported nitrate reduction at -0.30 V vs Ag/AgCl (-103 mV vs SHE) at pH 8 and 22ºC in a cathode predominantly covered by the *betaproteobacteria Thiobacillus* sp. Additionally, Gregoire et al. (Gregoire et al., 2014) exhibited a biocathode predominantly covered by the *betaproteobacteria Rhodocyclales* and *Burkholderiales* presenting nitrate reduction at -0.125 V vs Ag/AgCl (+72 mV vs SHE) at pH 7.2 and 30ºC.

From the results obtained, it can be suggested that the electroactive biofilm developed on the working electrodes was capable of switching from an anodic to a cathodic state. Interestingly, when comparing the similarity of formal potential values of i) acetate-oxidizing and ii) nitrate-reducing conditions in this study, it can be suggested that, from an electrochemical perspective, a similar electron transfer mechanism should be used for both purposes (anodic and cathodic behaviour) (Rosenbaum et al., 2011).

3.2.2. Non-turnover CV and DPV analyses of cathodic biofilms

After complete conversion of nitrate into dinitrogen, the biofilm was again tested under non-turnover conditions (Fig. 3B, blue CV and Fig. 2C, blue DPV). In this case, the CV depicted a clearer redox couple around -158±33 mV. The application of DPVs confirmed the predominance of the redox couple found in CV with a formal potential ($E_{f,1}$) at -158±33 mV. Additionally, a “shoulder” in DPV that resembled somehow a

peak around +183±2 mV was found. However, it remains unclear how the peak with formal potential $E_{f,2}$ could participate in the overall ET mechanism.

Additionally, the shape observed in cathodic non-turnover CVs presented a lower capacitance. An increase of capacitance in CV has been associated with the growth of an electroactive biofilm on the electrode surface (Schrott et al., 2011). Therefore, the decrease of capacitance in CVs under non-turnover cathodic vs. anodic conditions could indicate that only a certain percentage of the biofilm was able to catalyze the reduction of nitrate. The loss of capacitance in cathodic non-turnover CV also illustrates that some microorganisms within the biofilm were not active in such conditions.

When considering all the formal potentials calculated under both anodic and cathodic conditions, it is evident that no significant shift of the formal potentials for acetate oxidation and nitrate reduction exists. Therefore, from the electrochemical perspective, we suggest that the redox systems detected at a formal potential around -175 mV ($E_{f,1}$) were responsible for both delivering and taking electrons to and from the electrode, respectively. Nevertheless, from the microbiological perspective, whether the same electron transfer conduit is used for both acetate-oxidation and nitrate-reduction processes remains unclear and it would require more in-depth molecular studies evaluating the different cytochromes/proteins involved in both processes.

In a biosensor application, the developed biofilm would allow the detection of both acetate and nitrate. Although both catalytic processes presented a similar formal potential, acetate oxidation occurred at potentials higher than -175 mV, while nitrate reduction occurred at potentials below -175 mV. Therefore, the analysis of both compounds could be discerned by poising the working electrode at +397 mV for acetate and -303 mV for nitrate analyses, respectively.

3.3. Microbial biofilm analysis

3.3.1 Enrichment of *Geobacter* species

Similar bands were observed in both R1 and R2 replicates through PCR-DGGE analyses. Only the bands from R-1 were sequenced (Fig. 4) and subsequently quantified. In order to quantify the DGGE bands, these were stained and analyzed through ImageJ software (Supplementary material S6).

In samples taken after bioanodic conditions, bands A2→C2 presented the highest intensity (16.8% of abundance, supplementary material S6). Sequences retrieved from bands A2→C2 confirmed the presence of a *Geobacter* species with (> 99% similarity with *Geobacter* sp. CLFeRB, Genbank accession number DQ086800). On the one side, several bacteria within the *Geobacteraceae* family are known to use an electrode as electron acceptor (anodic role) (Lovley et al., 2011). On the other side, nitrate reduction using the electrode as electron donor (cathode role) has only been confirmed for *Geobacter metallireducens* as a pure culture (Gregory et al., 2004), and a mixed bacterial community enriched in *Geobacter grbiciae* (Gregory et al., 2004).

Despite *Geobacter* sp. str. CLFeRB (99%) has been recently described to develop on BES anodes (Jung and Regan, 2007; Zhang et al., 2014), its capability for nitrate reduction is still unknown. According to phylogenetic inferences with known and physiologically characterized *Geobacter* species (Fig. 4), A2→C2 sequences had high similarities to the 16S rRNA gene sequence of *Geobacter pelophilus* Dfr2 (95%) and *Geobacter argillaceus* G12 (73%). Both species are able to use acetate as electron donor (Lovley et al., 2011; Straub and Buchholz-Cleven, 2001) and nitrate as electron acceptor (Lovley et al., 2011; Ohtsuka et al., 2013) and have been detected in anode biofilms but not in denitrifying cathodes (de Cárcer et al., 2011; Kouzuma et al., 2013). Hence we show, for the first time, the presence of this bacterium in anodes and cathodes

at relevant cells densities. The enrichment of *Geobacter* sp. on the working electrode surface was very likely due to the constant experimental conditions imposed throughout the experiments, such as: (i) the use of a fixed anodic applied potential (+397 mV vs. SHE), (ii) constant temperature (22°C), (iii) neutral pH (7.0), (iv) homogeneous mass transfer in the bulk medium due to continuous stirring, (iv) use of a synthetic medium containing a non fermentable substrate, such as acetate and (v) strict anoxic conditions (Harnisch et al., 2011; Liu et al., 2008; Yates et al., 2012).

After the switching to cathodic conditions, the most intense band was still the band belonging to *Geobacter* sp. (band A2→C2; 27.4% band relative abundance), suggesting that the cathodic activity was very likely due to this microorganism and thus the main responsible of the bidirectional microbial electron transfer using redox systems with formal potential at around -175 mV ($E_{f,1}$). No voltammetric analyses of bidirectional electron transfer behaviour for anodic acetate-oxidation coupled with cathodic nitrate-reduction had been reported previously, and reduction reactions are restricted to the use of fumarate as an electron acceptor. Dumas et al. (2008) and Strycharz et al. (2011) evaluated the bidirectional activity of *Geobacter sulfurreducens* for anodic acetate-oxidation and cathodic fumarate-reduction. Their results suggested that electrons for anodic acetate oxidation and cathodic fumarate reduction in pure cultures were transferred using different electron conduits. The differences observed for bidirectional activity of acetate-oxidation/nitrate-reduction (this study) compared to acetate-oxidation/fumarate-reduction (Dumas et al., 2008; Strycharz et al., 2011) could be explained by the nature of the electron acceptor as well as the different experimental set-up used. It is worth noticing that nitrate and fumarate formal potentials are significantly different. At pH 7, fumarate/succinate formal potential is +33 mV vs SHE, while nitrate/nitrite formal potential is +424 mV vs SHE. Moreover, in the present

study, a mixed culture biofilm was characterized and thus the observed formal potential indicates a mean value for the whole mixed culture biofilm, not only for a single bacterial specie.

3.3.2 Less abundant members of the electrode microbial community

Other less intense bands showed relevant changes in their relative intensity when electrode was switched from anodic to cathodic conditions, thus revealing some specificity on prevailing bacterial metabolisms.

DGGE bands A1→C1 and A3→C3 decreased during cathodic conditions compared to anodic conditions (Supplementary material S6). Interestingly, sequence from band A3→C3 that clustered within the *Rhodocyclaceae* (*betaproteobacteria*), a family containing several denitrifying species, disappeared when switching from anodic (A3) to cathodic (C3) conditions (from 16.7 to 0.0%). These results suggest that, although present in anodic conditions, this bacterial phylotype is not likely to participate in electrocatalytic nitrate reduction since it is wiped out from the electrode due to the less favorable conditions.

The *deltaproteobacteria Desulfobrivio* sp. (bands A5→C5) presented a similar intensity in both conditions (2.7 and 3.0% in terms of band relative abundance), which could indicate that was capable of living in both environments.

Sequence from band A4→C4 showed relevant similarities to members of the *Synergistetes* group. They increased on intensity as conditions were switched from anodic to cathodic (from 2.0 to 26.0%), suggesting that cathodic conditions were more favorable for this microorganism, allowing them to grow. Members of *Synergistetes* group has been found in nitrifying and denitrifying reactors (Wang et al., 2014) and some are known to perform sulfide dependent nitrate reduction (Cytryn et al., 2005). It supports the growth of *Synergistetes* under nitrate reducing conditions.

Besides different contribution of the less abundant members was detected in anodic acetate-oxidizing (*Geobacter* dominance shared with *Rhodocyclaceae*) and cathodic nitrate-reducing conditions (*Geobacter* dominance shared with *Synergistetes*), a similar redox system at -175 mV ($E_{f,1}$) was detected in CVs and DPVs, suggesting that the main contributor to the catalytic signal was similarly present in both conditions. Therefore, a mixed culture biofilm predominantly composed by *Geobacter* sp. was responsible of the bidirectional microbial electron transfer using redox systems with formal potential at around -175 mV ($E_{f,1}$).

The results obtained in this study also have an impact on the study of autonomous microbial fuel cells (i.e., electricity can be obtained from spontaneous redox processes) that couple acetate oxidation and nitrate reduction (Clauwaert et al., 2009). The results presented here suggest that an acetate-oxidizing anode and a nitrate-reducing cathode composed of *Geobacter* sp. dominated biofilms would not produce a thermodynamic spontaneous process. In fact, the enrichment of *Geobacter* sp. in denitrifying biocathodes have been reported when operating the cathode at a poised potential (Gregory et al., 2004), but not under microbial fuel cell mode.

4. CONCLUSIONS

In this study we report (based) on the electrochemical characterization of a "switchable" electroactive biofilm. A microbial community predominantly composed by *Geobacter* sp. was able to both oxidize acetate at a poised electrode potential of +397 mV and reduce nitrate at -303 mV. Voltammetric analyses revealed that electron transfer for both acetate oxidation and nitrate reduction took place at a similar formal potential, thus carried out by the same consortia. Biocatalysis of acetate occurred at a formal potential of -175±5 mV while nitrate reduction occurred at a formal potential of -175±34 mV (vs. SHE). With non-turnover cyclic voltammetry formal potentials of -159±22 and -158±33

mV were calculated in bioanodic and biocathodic conditions, respectively. These results suggest that the electroactive biofilm was capable of switching its activity from an anodic acetate-oxidizing state to a cathodic nitrate-reducing state by using an electron channel located at around a redox potential of -175 mV in both cases.

The results presented here pave the way on the investigation of switchable electroactive biofilms. Not only the same biofilm can be operated as anode or as a cathode, but also the same electron transport conduit can be used for both purposes.

ACKNOWLEDGEMENTS

This work was supported by the Spanish Government (CTQ2014SGR-1168, CTQ2014-53718-R). A.A.C.M. was supported by the French National Research Agency (Project: ANR-10-BTBR-02). N.P. was supported by the Catalan Government (2012FI-B00941). The authors acknowledge the scientific contribution of Pau Batlle-Vilanova (LEQUIA-UdG).

5. REFERENCES

APHA, 2005. Standard Methods for the Examination of Water and Wastewater, 19th ed. Washington DC, USA.

Baron, D., LaBelle, E., Coursolle, D., Gralnick, J.A., Bond, D.R., 2009. J. Biol. Chem. 284 (42), 28865–28873. doi:10.1074/jbc.M109.043455.

Batlle-Vilanova, P., Puig, S., Gonzalez-Olmos, R., Vilajeliu-Pons, A., Bañeras, L., Balaguer, M.D., Colprim, J., 2014. Int. J. Hydrogen Energy 39 (3), 1297–1305. doi:10.1016/j.ijhydene.2013.11.017.

Blanchet, E., Pécastaings, S., Erable, B., Roques, C., Bergel, A., 2014. Bioresour. Technol. 173, 224–30. doi:10.1016/j.biortech.2014.09.076.

Bond, D.R., Lovley, D.R., 2003. Appl. Environ. Microbiol. 69 (3), 1548–1555. doi:10.1128/AEM.69.3.1548-1555.2003.

Carmona-Martinez, A.A., Harnisch, F., Fitzgerald, L.A., Biffinger, J.C., Ringeisen, B.R., Schröder, U., 2011. Bioelectrochemistry 81 (2), 74–80. doi:10.1016/j.bioelechem.2011.02.006.

Carmona-Martínez, A.A., Pierra, M., Trably, E., Bernet, N., 2013. Phys. Chem. Chem. Phys. 15 (45), 19699–19707. doi:10.1039/c3cp54045f.

Cheng, K.Y., Ginige, M.P., Kaksonen, A.H., 2012. Environ. Sci. Technol. 46 (18), 10372–10378. doi:10.1021/es3025066

Cheng, K.Y., Ho, G., Cord-Ruwisch, R., 2010. Environ. Sci. Technol. 44 (1), 518–525. doi:10.1021/es9023833

Clauwaert, P., Rabaey, K., Aelterman, P., De Schamphelaire, L., Pham, T.H., Boeckx, P., Boon, N., Verstraete, W., 2007. Environ. Sci. Technol. 41 (9), 3354–3360. doi:10.1021/es062580r.

Cytryn, E., Van Rijn, J., Schramm, A., Gieseke, A., De Beer, D., Minz, D., 2005. Appl. Environ. Microbiol. 71 (10), 6134–6141. doi:10.1128/AEM.71.10.6134-6141.2005.

De Cárcer, D.A., Ha, P.T., Jang, J.K., Chang, I.S., 2011. Appl. Microbiol. Biotechnol. 89 (3), 605–12. doi:10.1007/s00253-010-2903-x.

Dumas, C., Basseguy, R., Bergel, A., 2008. Electrochim. Acta 53 (5), 2494–2500. doi:10.1016/j.electacta.2007.10.018.

Fourmond, V., Hoke, K., Heering, H.A., Baffert, C., Leroux, F., Bertrand, P., Léger, C., 2009. Bioelectrochemistry 76 (1-2), 141–147. doi:10.1016/j.bioelechem.2009.02.010.

Fricke, K., Harnisch, F., Schröder, U., 2008. Energy Environ. Sci. 1 (1), 144–147. doi:10.1039/b802363h.

Ganigué, R., Puig, S., Batlle-Vilanova, P., Balaguer, M.D., Colprim, J., 2015. Chem. Commun. 51, 3235–3238. doi:10.1039/C4CC10121A.

Geelhoed, J.S., Stams, A.J.M., 2011. Environ. Sci. Technol. 45 (2), 815–820. doi:10.1021/es102842p.

Gimkiewicz, C., Harnisch, F., 2013. J. Vis. Exp. (82), 50800.

Gregoire, K.P., Glaven, S.M., Hervey, J., Lin, B., Tender, L.M., 2014. J. Electrochem. Soc. 161 (13), H3049–H3057. doi:10.1149/2.0101413jes

Gregory, K.B., Bond, D.R., Lovley, D.R., 2004. Environ. Microbiol. 6 (6), 596–604. doi:10.1111/j.1462-2920.2004.00593.x.

Harnisch, F., Freguia, S., 2012. Chem. Asian J. 7 (3), 466–475. doi:10.1002/asia.201100740.

Harnisch, F., Koch, C., Patil, S.A., Hübschmann, T., Müller, S., Schröder, U., 2011. Energy Environ. Sci. 4 (4), 1265–1267. doi:10.1039/c0ee00605j.

Harnisch, F., Rabaey, K., 2012. ChemSusChem 5 (6), 1027–1038. doi:10.1002/cssc.201100817.

Jeremiasse, A.W., Hamelers, H.V., Croese, E., Buisman, C.J., 2012. Biotechnol. Bioeng. 109 (3), 657–664. doi:10.1002/bit.24338.

1 Jung, S., Regan, J.M., 2007. Appl. Microbiol. Biotechnol. 77 (2), 393–402.
2 doi:10.1007/s00253-007-1162-y.

3 Kouzuma, A., Kasai, T., Nakagawa, G., Yamamuro, A., Abe, T., Watanabe, K., 2013.
4 PLoS One 8 (11), e77443. doi:10.1371/journal.pone.0077443.

5 Lane, D.J., 1991. 16S/23S rRNA sequencing, in: Sons, J.W. and (Ed.), Nucleic acid
6 techniques in bacterial systematic. New York, USA, pp. 115-175.

7 Liu, Y., Harnisch, F., Fricke, K., Sietmann, R., Schröder, U., 2008. Biosens.
8 Bioelectron. 24 (4), 1012–1017. doi:10.1016/j.bios.2008.08.001.

9 Logan, B.E., 2012. ChemSusChem 5 (6), 988–994. doi:10.1002/cssc.201100604.

10 Logan, B.E., Rabaey, K., 2012. Science 337 (6095), 686–690.
11 doi:10.1126/science.1217412.

12 Lovley, D.R., 1991. Microbiol. Rev. 55 (2), 259-287.

13 Lovley, D.R., Ueki, T., Zhang, T., Malvankar, N.S., Shrestha, P.M., Flanagan, K.A.,
14 Aklujkar, M., Butler, J.E., Giloteaux, L., Rotaru, A.-E., Holmes, D.E., Franks, A.E.,
15 Orellana, R., Risso, C., Nevin, K.P., 2011. Geobacter: the microbe electric's
16 physiology, ecology, and practical applications., 1st ed, Advances in microbial
17 physiology. Elsevier Ltd. doi:10.1016/B978-0-12-387661-4.00004-5.

18 Marsili, E., Baron, D.B., Shikhare, I.D., Coursolle, D., Gralnick, J.A., Bond, D.R.,
19 2008. Proc. Natl. Acad. Sci. U. S. A. 105 (10), 3968–3973.
20 doi:10.1073/pnas.0710525105.

Ohtsuka, T., Yamaguchi, N., Makino, T., Sakurai, K., Kimura, K., Kudo, K., Homma, E., Dong, D.T., 2013. Environ. Sci. Technol. 47 (12), 6263-6271. doi: 10.1021/es400231x.

Pant, D., Singh, A., Van Bogaert, G., Irving Olsen, S., Singh Nigam, P., Diels, L., Vanbroekhoven, K., 2012. RSC Adv. 2 (4), 1248–1263. doi:10.1039/c1ra00839k.

Parameswaran, P., Bry, T., Popat, S.C., Lusk, B.G., Rittmann, B.E., Torres, C.I., 2013. Environ. Sci. Technol. 47 (9), 4934–4940. doi:10.1021/es400321c.

Pous, N., Koch, C., Colprim, J., Puig, S., Harnisch, F., 2014. Electrochem. commun. 49, 93–97. doi:10.1016/j.elecom.2014.10.011.

Pous, N., Puig, S., Dolors Balaguer, M., Colprim, J., 2015. Chem. Eng. J. 263, 151–159. doi:10.1016/j.cej.2014.11.002.

Prat, C., Ruiz-Rueda, O., Trias, R., Anticó, E., Capone, D., Sefton, M., Bañeras, L., 2009. Appl. Environ. Microbiol. 75 (7), 1922-1931. doi: 10.1128/AEM.02758-08.

Rosenbaum, M., Aulenta, F., Villano, M., Angenent, L.T., 2011. Bioresour. Technol. 102 (1), 324–333. doi:10.1016/j.biortech.2010.07.008.

Ross, D.E., Flynn, J.M., Baron, D.B., Gralnick, J.A., Bond, D.R., 2011. PLoS One 6 (2), e16649. doi:10.1371/journal.pone.0016649.

Schröder, U., 2007. Phys. Chem. Chem. Phys. 9 (21), 2619–2629. doi:10.1039/b703627m.

Schrott, G.D., Bonanni, P.S., Robuschi, L., Esteve-Nuñez, A., Busalmen, J.P., 2011. Electrochim. Acta 56 (28), 10791–10795. doi:10.1016/j.electacta.2011.07.001.

Shi, L., Rosso, K.M., Zachara, J.M., Fredrickson, J.K., 2012. Biochem. Soc. Trans. 40 (6), 1261–1267. doi:10.1042/BST20120098.

Straub, K.L., Buchholz-Cleven, B.E.E., 2001. Int. J. Syst. Evol. Microbiol. 51 (5), 1805–1808.

Strycharz, S.M., Glaven, R.H., Coppi, M.V, Gannon, S.M., Perpetua, L.A, Liu, A., Nevin, K.P., Lovley, D.R., 2011. Bioelectrochemistry 80 (2), 142–150. doi:10.1016/j.bioelechem.2010.07.005.

Summers, Z.M., Gralnick, J.A., Bond, D.R., 2013. mBio 4 (1), e00420-00412.

Tamura, K., Stecher, G., Peterson, D., Filipski, A., Kumar, S., 2013. Mol. Biol. Evol. 30 (12), 2725–2729. doi:10.1093/molbev/mst197.

Turner, S., Pryer, K.M., Miao, V.P.W., Palmer, J.D., 1999. J. Eukaryot. Microbiol. 46 (4), 327-338.

Virdis, B., Rabaey, K., Yuan, Z., Rozendal, R.A., Keller, J., 2009. Environ. Sci. Technol. 43 (13), 5144–5149. doi:10.1021/es8036302.

Wang, Z., Zhang, X.-X., Lu, X., Liu, B., Li, Y., Long, C., Li, A., 2014. PLoS One 9 (11), e113603. doi:10.1371/journal.pone.0113603.

Xing, D., Zuo, Y., Cheng, S., Regan, J.M., Logan, B.E., 2008. Environ. Sci. Technol. 42 (11), 4146–4151. doi:10.1021/es800312v.

Yates, M.D., Kiely, P.D., Call, D.F., Rismani-Yazdi, H., Bibby, K., Peccia, J., Regan, J.M., Logan, B.E., 2012. ISME J. 6 (11), 2002–2013. doi:10.1038/ismej.2012.42.

Zhang, H., Chen, X., Braithwaite, D., He, Z., 2014. PLoS One 9 (9), e107460. doi:10.1371/journal.pone.0107460.

Highlights

- Growth of electroactive biofilm able to oxidize acetate and reduce nitrate.
- Electrochemical characterization of the switchable electroactive biofilm.
- Bidirectional catalysis using a redox system located around -175 mV vs. SHE.
- Biofilm predominantly composed of *Geobacter* sp.

Table 1. Summary of electrochemical data extracted from CVs and DPVs.

WE role	$E_{app.}$ (mV vs. SHE)	**Conditions**	E_f (mV vs. SHE)
Anode	+397	Turnover	-175±05
		Non-turnover	-159±22
Cathode	-303	Turnover	-175±34
		Non-turnover	-158±33

WE: working electrode; E_{app}: applied potential during chronoamperometry; E_f: formal potential. Note: Turnover and Non-turnover conditions indicate the presence (turnover) or absence (non-turnover) of substrate while performing voltammetric analyses in anodic (acetate) and cathodic (nitrate) conditions.

Figure_1

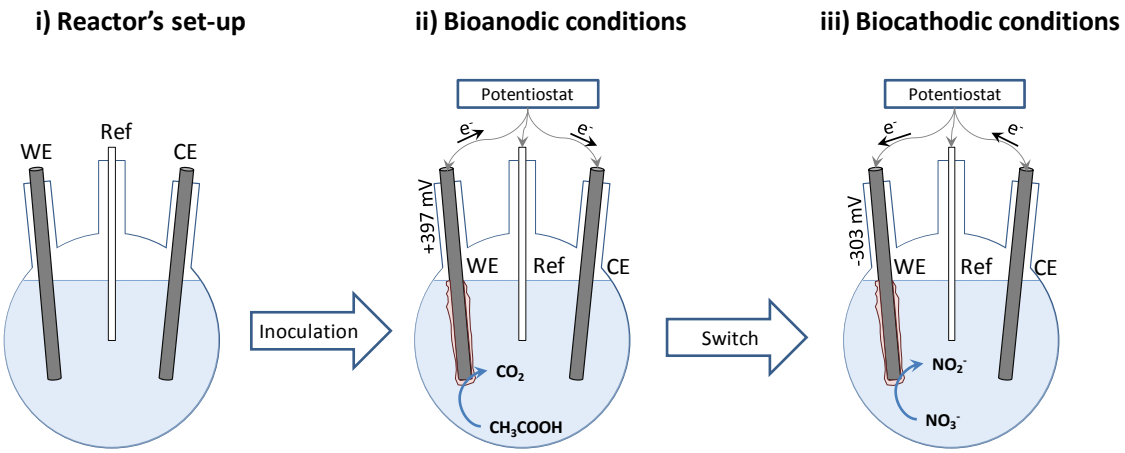

Figure 1. Scheme of the reactor's configuration used to perform the studies as well as the workflow followed: i) Reactor's set-up; ii) bioanodic conditions and iii) biocathodic conditions.

Figure_2

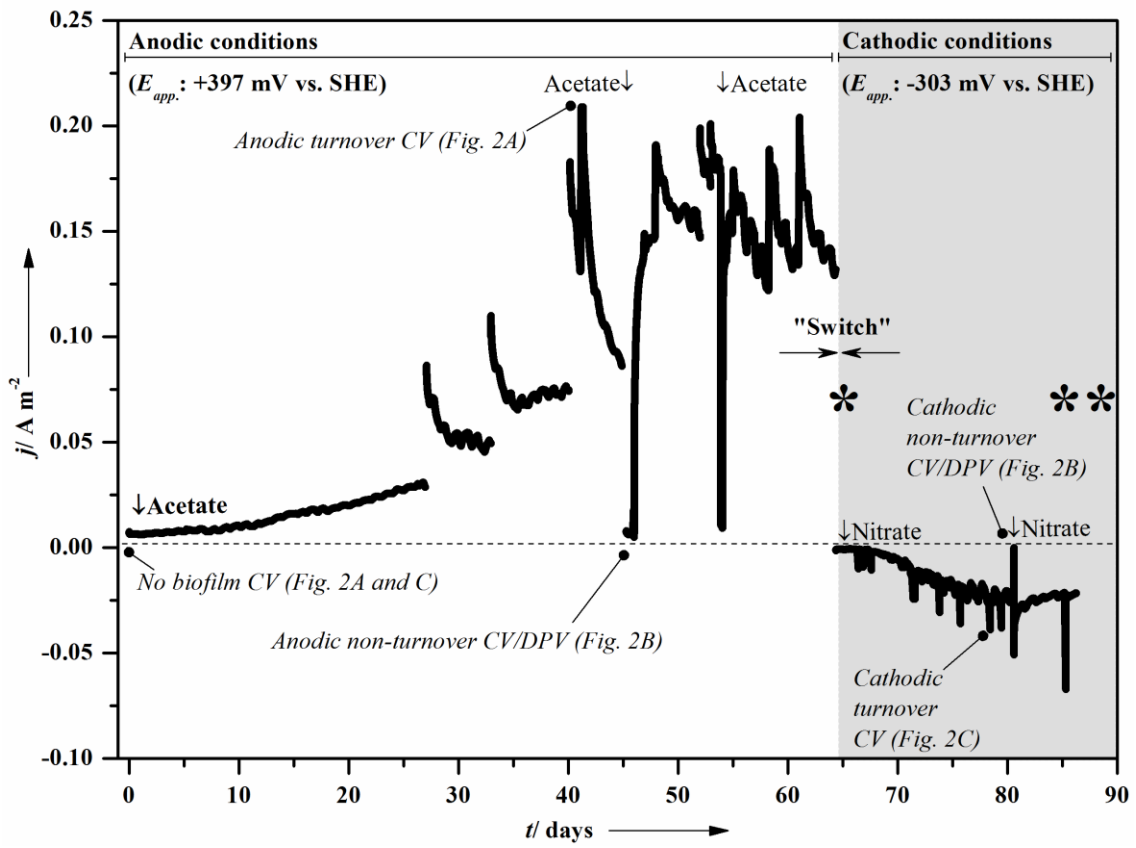

Figure 2. Overall strategy of biofilm formation and electrochemical characterization points. Exemplary chronoamperometry for R-2 is shown. Sampling for microbial analyses after anodic (*) and cathodic (**) conditions are indicated. Vertical arrows indicate addition of acetate (206 ppmC-CH_3COO^-, anodic conditions) or nitrate (32 ppmN-NO_3^-; cathodic conditions).

Figure_3

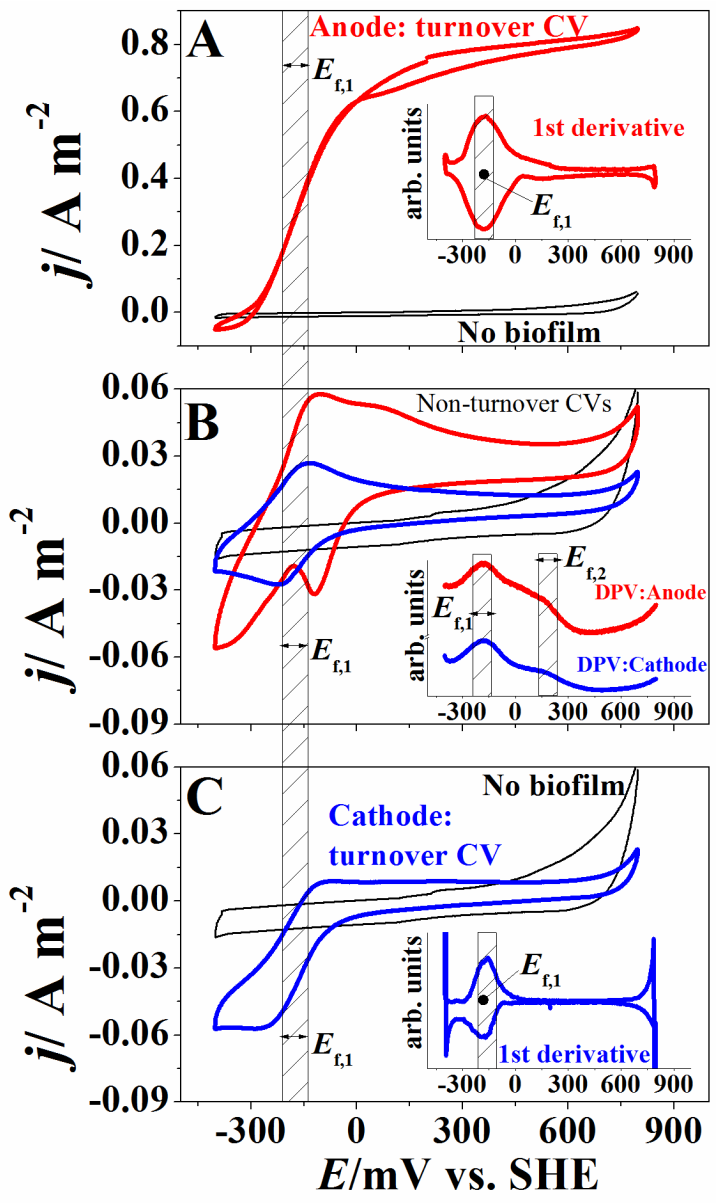

Figure 3. Representative voltammograms of a mature electroactive biofilm during anodic (red) and cathodic (blue) conditions. A) Anodic turnover CV (inset: first derivative); B) Non-turnover CVs (inset: DPVs) and C) Cathodic Turnover CV (inset: first derivative). Note: bare electrode CV in A, B and C shows the CV before biofilm growth (black).

Figure_4

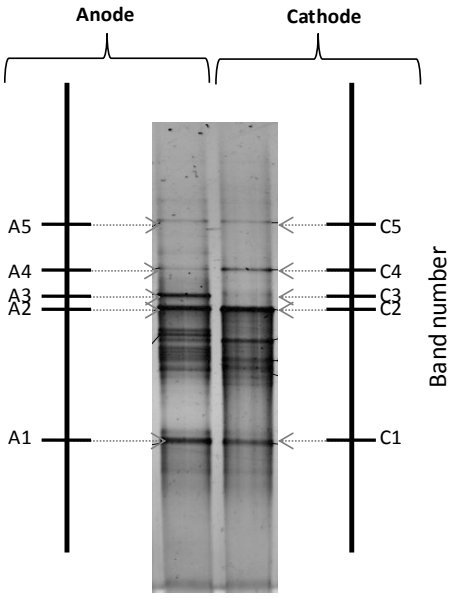

Sequenced bands	Taxonomy
A1-C1	*Bacteroidetes*
A2-C2	*Geobacter* sp.
A3-C3	*Rhodocyclaceae*
A4-C4	*Synergistetes*
A5-C5	*Desulfovibrio* sp.

Figure 4. DGGE profiles of the microbial community within the biofilm after anodic and cathodic conditions in R-1 sample. Taxonomic information according to BLAST searches of analyzed sequences is summarized in the table at the right side.

Figure_5

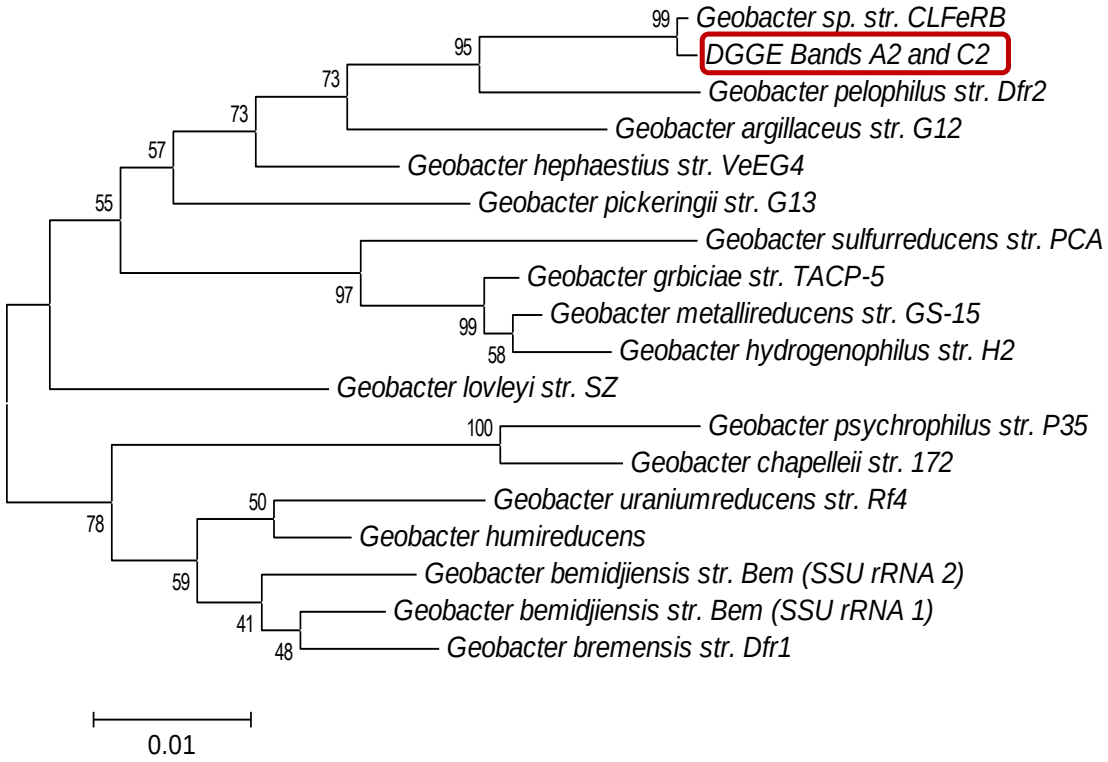

Figure 5. Phylogenetic analysis based on 16S rRNA gene sequence obtained in this study (DGGE Bands A2→C2) is marked in red. Sequences and accession numbers of selected organisms were retrieved from GenBank. Phylogenetic distances were determined by neighbor-joining method.